PHASE TRANSITION SIGNALS IN HEAVY ION COLLISIONS BY LATINO MODEL

A. BARRAÑÓN[1], J.A. LÓPEZ-GALLARDO[2], F. de L. CASTILLO-ALVARADO[3]

Abstract. LATINO Model is a semi-classical approach to simulate heavy ion collisions attaining qualitative and quantitative agreement with theoretical predictions and experimental results. Criticality signals have been obtained in this study where impact parameter and projectile energy are increased. Large density fluctuations are described by large values of the relative variance plotted in Campi Plots. Self-similarity in the critical region is signed by linear plots of Scaled Factorial Moments. These signatures are related to a liquid gas phase transition for nuclear matter. Also Excitation curves and Temperature plateau decrease with residual size in agreement with experimental results.

Key words: heavy ion collisions, statistical signatures, criticality.

1. INTRODUCTION

Heavy Ion Collisions are expected to experience a liquid-gas phase transition due to the specifics of the internucleonic interaction, which is attractive in both the long and intermediate ranges and repulsive in the short range. It is possible that a wide zone of phase space is explored when two nuclei collide, including a region where liquid and gas phases coexist, namely the spinodal region. At this spinodal region, incompressibility is negative and uniform nuclear matter is unstable, leading to multifragmentation due to the increase of density fluctuations [1, 2]. LATINO Model includes all correlations while dynamical simulations based on Boltzmann equation, such as Landau-Vlasov (LV), Boltzmann-Uehling-Uhlenbeck (BUU) or Boltzmann-Nordheim-Vlasov (BNV), describe the time evolution of the density of a one-body system, ignoring those correlations whose order is larger than the order of binary correlations, neglecting fluctuations around the mean trajectory of the system, which altogether comes out to be quite inconvenient to study the spinodal instability zone [10]. As shown by Guarnera *et al.* [3], a spinodal decomposition produces a "primitive breakup" where equal sized fragments have a privileged fragment size, which is related to the wave lengths of the most unstable modes of nuclear matter.

[1] Department of Basic Sciences, UAM-Azcapotzalco, Mexico D.F., Mexico
[2] Department of Physics, University of Texas-El Paso, TX, USA
[3] Department of Physics, ESFM-IPN, Mexico D.F., Mexico, Phone (55) 5318-9015, Fax (55) 5318-954, E-mail: bca@correo.azc.uam.mx

Tabacaru *et al*. have obtained reduced velocity correlations between fragments and did not find a bubble-like profile, which excludes surface instabilities that might cause multifragmentation. They also computed higher order charge correlations, defined as the ratio between the number of correlated fragments and the number of uncorrelated fragments, obtaining evidence of a privileged production of equal sized fragments. Chomaz *et al*. [4] have introduced a scenario inspired on experimental data, where a gently compressed systems expands and reaches thermal equilibrium approximately at the time when system enters into the spinodal region. At this moment, density fluctuations break up the system into several hot fragments and particles. When fragments are released from the nuclear force, configuration frozen and fragments only interact with each other via Coulomb force. At this moment, system has explored so much phase space that it can be described by statistical models and there is no contradiction between statistical or dynamical approximations. Barrañón *et al*. have obtained computational evidence about the inverse relation between entropy and the residual size, using LATINO dynamical model to study the spinodal decomposition region of central HIC at intermediate energies [5].

Until now, several criticality signals have been essayed for Heavy Ion Collisions. M. D'Agostino *et al*., obtained a signal of criticality in terms of the negative sign of the heat capacity which resists several kinds of calorimetric reconstruction from experimental data [6]. In the experimental field a power law for the intermediate fragments distribution has been interpreted as a signal of the proximity to the critical point of the liquid-gas phase transition. J.B. Elliott *et al*. [7] have used the liquid droplet model to estimate the critical temperature with a value close to 6.7 MeV. And other authors have analysed Campi plots to prove that phase transition happens at the spinodal decomposition, calling this very temperature a spinodal critical temperature Tc, with a value close to 6 MeV [8].

Many studies have been performed to describe the phase transitions in Heavy Ion Collisions in terms of statistical and dynamical models. Critical temperatures are in the range of 5–20 MeV/A, and size dependence has been observed since many years ago. LATINO Model is a semi-classical model that takes on account dynamical evolution of these Heavy Ion Collisions and provides statistical information of fragmentation. This way, statistical signatures can be used to detect critical behavior and dynamical effects can also be replicated. In the following sections we show several statistical signatures of criticality for Heavy Ion Collision simulated via LATINO Model. In this very study some statistical evidence is reported about a liquid-gas phase transition. Other features of Heavy Ion Collisions behavior have been computationally replicated and hereby reported, namely the dependence of excitation with size system as well as the dependence of limit temperatures with system size. LATINO Model has been used elsewhere to provide computational evidence concerning dynamical instabilities associated with phase transitions due to spinodal decomposition which is in agreement with experimental observations [5, 10], and a signature of breakups with fragments of

equal size is hereby computed which indicates a spinodal decomposition as a source of this critical behavior.

2. METHODOLOGY

Heavy Ion collisions were simulated using LATINO semi-classical model where binary interaction is reproduced with a Pandharipande potential given by:

$$V_{nn} = V_{pp} = V_0 \left(\frac{e^{-\mu_0 r}}{r} - \frac{e^{-\mu_0 r_C}}{r_C} \right) \tag{1}$$

and

$$V_{np} = V_r \left(\frac{e^{-\mu_r r}}{r} - \frac{e^{-\mu_r r_C}}{r_C} \right) - V_a \left(\frac{e^{-\mu_a r}}{r} - \frac{e^{-\mu_a r_a}}{r_a} \right) \tag{2}$$

made up from linear combinations of Yukawa potentials, where

$$\mu_r = 1.7468 \frac{1}{\text{fm}}, \mu_0 = 1.5 \frac{1}{\text{fm}}, \mu_a = 1.6 \frac{1}{\text{fm}}, V_0 = 373.118 \text{ MeV}, \tag{3}$$

$$V_r = 3088.118 \text{ MeV}, \tag{4}$$

and

$$V_a = 2666.647 \text{ MeV}. \tag{5}$$

These coefficients are designed to allow the potential to fulfill the properties of nuclear matter in ground state and to comply with Pauli Exclusion Principle [10, 11]. This potential provides a equation of state that has an isothermal compressibility K in the range of 250 MeV, where:

$$K = n \left(\frac{\partial p}{\partial n} \right)_T \tag{6}$$

and amazingly reproduces the properties of nuclear matter in ground state since its equilibrium density is equal to $\rho_0 = 0.16 \text{ fm}^{-3}$ with and energy $E(\rho_0)$ equal to -16 MeV/nucleon.

Clusters are detected using an Early Cluster Recognition Algorithm that optimizes the configurations in energy space. Most Bound Partition is obtained minimizing the sum of cluster energies for each partition:

$$\{C_i\} = \arg\min\left[E_{\{C_i\}} = \sum_i E_{\text{int}}^{C_i}\right], \tag{7}$$

where the cluster energy is given by:

$$E_{\text{int}}^{C_i} = \sum_i \left[\sum_{ij \in C_i} K_j^{CM} + \sum_{j,k \in C_{iu}, j \leq k} V_{jk}\right] \tag{8}$$

in this expression the first sum is on the partition clusters, K_j^{CM} is the kinetic energy of particle j measured in the cluster mass centre, and V_{ij} is the internucleonic potential. The algorithm uses the technique of "simulated annealing" to find the most bound partition in energy space.

   Ground states of neutron or proton rich sources, were built up starting from a random configuration with a given kinetic energy and confined in a parabolic potential (Fig. 1). Nucleon speed was gradually reduced until the system was bound, afterwards the parabolic potential was suppressed and a frictional method was applied until the system reached its theoretical binding energy.

   Projectile is boosted on target with a given kinetic energy for distinct impact parameters. System evolution was simulated using a Verlet algorithm [12], where two Taylor expansions are subtracted, one of them forwards and the other backwards on time:

$$\vec{r}(t + \Delta t) = 2\vec{r}(t) - \vec{r}(t - \Delta t) + \vec{a}(t)h^2, \tag{9}$$

$$\vec{v}(t + \Delta t) = \vec{v}(t) + 0.5 * \left[\vec{a}(t + \Delta t) + \vec{a}(t)\right]h, \tag{10}$$

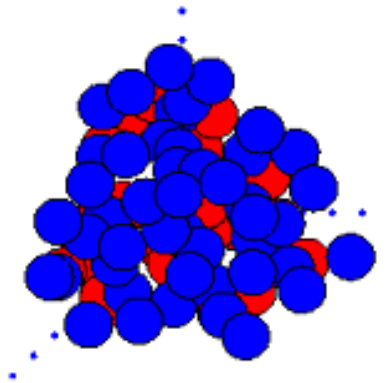$$\vec{a}(t + \Delta t) = -(1/m)\nabla V\left(\vec{r}(t + \Delta t)\right). \tag{11}$$

Fig. 1 – Ground State of the heavy ion Zn^{76} obtained starting from a random configuration, subsequently confined in a parabolic potential and finally cooled by a frictional method until it attains the theoretical binding energy.

Projectile energy is varied in the range going from 600 up to 2 000 MeV and system evolves until its microscopic composition remains frozen (Fig. 2), although some monomers might be ejected.
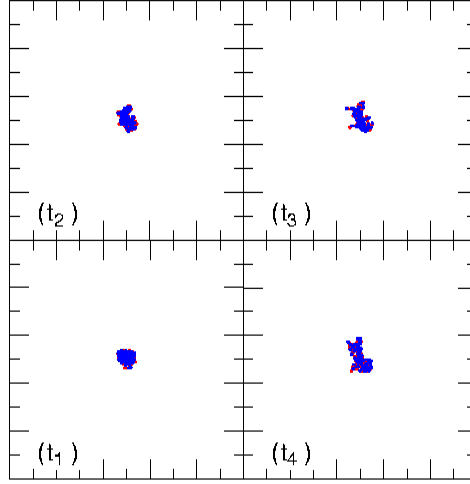

Fig. 2 – Time evolution of a heavy ion collision simulated with LATINO Model.

This time can be determined using the Microscopic Persistence Coefficient, defined as the probability of having two particles linked in a cluster of partition X still bound in a cluster of partition Y:

$$P[X,Y] = \frac{1}{\sum\limits_{cluster} n_i} \sum\limits_{cluster} n_i a_i / b_i \; , \tag{12}$$

where b_i is equal to the number of particles that belong to cluster C_i of partition $X \equiv \{C_i\}$ and a_i is equal to the number of particle pairs belonging to cluster C_i of partition $X \equiv \{C_i\}$ that also belong to a given cluster C_i' of partition $Y \equiv \{C_i'\}$. n_i is the number of particles in cluster C_i. Persistence attains an asymptotic limit value once the biggest fragment size (BFS), as well as the logarithmic derivative of the kinetic energy transported by light fragments and the logarithmic derivative of the number of intermediate fragments are altogether stable.

It is convenient to study the time evolution of the following quantities defined in terms of the last persistence. Namely forwards persistence:

$$P^+[X(t)] \equiv P[X(t), X(t \to \infty)] / \langle P[X(t), X'(t \to \infty)] \rangle_{colisiones}. \tag{13}$$

Also a backwards persistence can be defined:

$$P^-[X(t)] \equiv P[X(t \to \infty), X(t)] / \langle P[X(t), X'(t)] \rangle_{colisiones} \qquad (14)$$

another way of defining the persistence to measure the instantaneous evolution persistence is:

$$P^{it}[X(t)] \equiv P[X(t), X(t+dt)] / \langle P[X(t+dt), X'(t+dt)] \rangle_{colisiones}, \qquad (15)$$

where $X(t)$ represents a partition computed at time t, $X(t \to \infty)$ is an asymptotic partition, $\langle \ \rangle_{colisiones}$ represents an average taken on the total set of collisions. $X'(t)$ is a partition identical to partition $X(t)$, except for a nucleon evaporated in each cluster. Fig. 3 shows how the backward and forward persistence attain a maximum value when the biggest fragment size (Mass) is decreased due to fragmentation along time. Also, Multiplicity, which is equal to the number of fragments, increases with time due to disassembling of the system. Persistence is related to the microscopic composition of the system which is frozen in the asymptotic region of time.
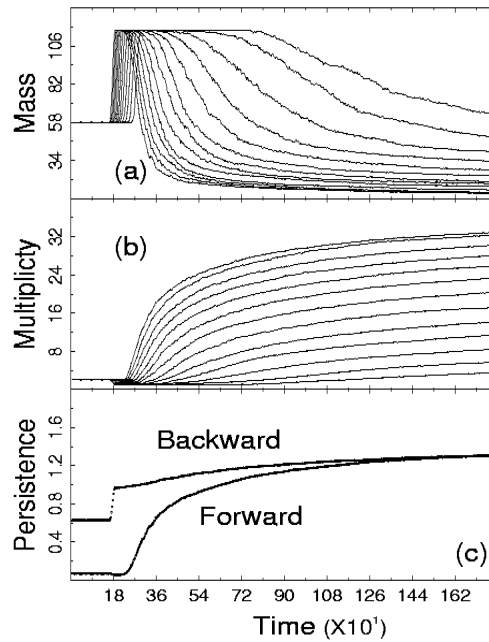

Fig 3 – Persistence in terms of Multiplicity and biggest fragment size.

Two colliding stages are observed, with an initial highly colliding stage produced when the projectile hits the droplet surface and the energy is distributed

chaotically. Collisions at this initial stage form a shock wave responsible for the prompt emission of light energetic particles from the surface. As the shock wave travels into the droplet, it produces density fluctuations and internal fractures. These are consequence of the momentum transferred and initiates disordered collisions leading to an excitation thermalization. Momentum transferred can be measured by Mean velocity transfer (MVT) which is given by:

$$\text{MVT}_i = \sum_k \left| V_{k,i}(t+dt) - V_{k,i}(t+dt) \right| \tag{16}$$

The first stage ends with a peak in the kinetic energy transported by promptly emitted light particles, signed by a peak in the KE(PEP) curve. A second stage ends with the attenuation of the intermediate size fragments production (IMF curve). Between these peaks of KEP(PEP) curve and IMF(curve), a peak in Mean Velocity Transfer (MVT curve) is observed. Hence, Mean Velocity Transfer (MVT) is increased due to the instabilities arising from the emission of prompt and fast light particles. As a result of these instabilities the compound fragment formed by the projectile and target, disassembles producing intermediate size fragments. MVT has been already stabilized before intermediate fragments are emitted inasmuch as the biggest fragment breaks up Fragments afterwards will freeze-out which can be signed by a sustained increase of the persistence. All these features are shown in Fig. 4.

Asymptotic fragment distributions are given by:

$$M_k^{(j)} = \sum_Z Z^k n^{(j)}(Z) / Z_{tot}, \tag{17}$$

when $k = 2$ this moment is proportional to the isothermal compressibility. Relative variance can be computed in terms of these moments and a high value of this variance indicates high density fluctuations:

$$\gamma = m_2 m_0 / m_1^2. \tag{18}$$

Chemical equilibrium is signed by the quantity: $\lambda = (n/p)\big|_{y>0} / (n/p)\big|_{y<0}$, where $(n/p)\big|_{y>0}$ and $(n/p)\big|_{y<0}$ are the quotients between the number of neutrons and protons moving forwards and backwards, respectively. And thermal equilibrium of the heavy residues can be examined studying the quadrupolar moment Q_{ZZ} defined by:

$$Q_{ZZ} = \int d\vec{r} d\vec{p} (2\pi)^3 \left[2p_z^2 - p_x^2 - p_y^2 \right] f(\vec{r}, \vec{p}, t), \tag{19}$$

where $f(\vec{r}, \vec{p}, t)$ is Wigner function. Clearly $Q_{ZZ} = 0$ is a sufficient condition for thermal equilibrium [26].
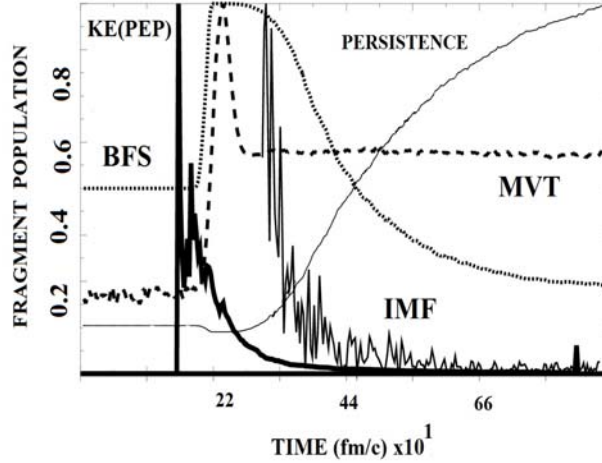

Fig. 4 – Shows how persistence grows with time.

Dynamical equilibrium is given when the squared adiabatic velocity is negative. This is given by:

$$V_c^2 = (1/m)\left[\left(\partial P/\partial\rho\right)_S\right] = (1/m)\left[\left(10/9\right) <E_K> + a\left(\rho/\rho_0\right) + b\left(\rho/\rho_0\right)^\sigma\right], \qquad (20)$$

where $<E_K>$ is the mean kinetic energy for nucleon, $a = -358.1$ MeV, $b = 304.8$ MeV and $\sigma = 7/6$ are the corresponding parameters of a soft equation of state. When $V_c^2 < 0$, nuclear matter is unstable with respect to density fluctuations which leads to dynamical instabilities.

Comparing the relaxation times for thermal, dynamical and chemical equilibrium, when the projectile energy is low, the largest relaxation time is the thermal one, since the energy is consumed by deformations and fragments are emitted from the surface (Fig. 2). But when the projectile energy is large, fragments are emitted from the bulk and therefore these relaxation times are the same (Fig. 5).

Fig. 6 shows a case where thermal and the chemical relaxation times are close to each other. As a matter of fact the isotopic temperature attains its asymptotic value in a very early stage of the collision even when the temperature of the biggest fragment is still changing as well as the size of the biggest fragment is still decreasing with time.
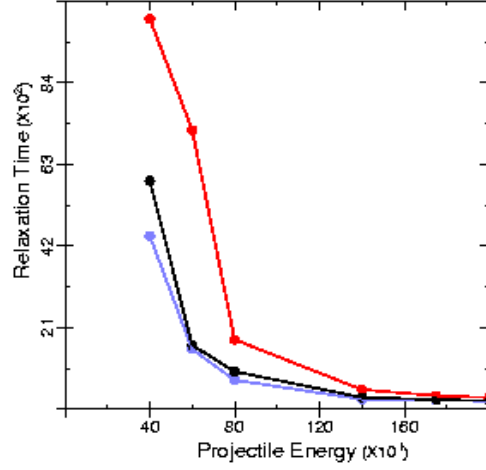
Fig. 5 – Relaxation times decrease with projectile energy for thermal, dynamical and chemical equilibrium in the case of central heavy ion collision Ni+Ni.
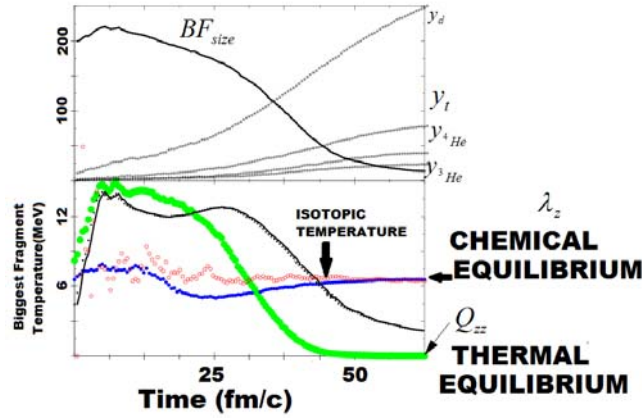

Fig. 6 – Relaxation times are in the same range for high values of the projectile energy.

The magnitude of the variance provides evidence of the closeness to the critical point. As a matter of fact, supposing that close to the critical point there is a general property of scaling and it comes out that in the neighborhood of the critical point [21]:

$$M_k \propto \left| T - T_C \right|^{-(1+k-\tau)/\sigma}, \tag{21}$$

when the multiplicity is critical in the case of heavy ion collisions, the following relation is fulfilled:

$$M_2 \propto \left| \varepsilon \right|^{-\gamma}, \tag{22}$$

therefore the relative variance comes out to be a reliable signal of criticality in heavy ion collisions. Campi Plots [22] use logarithmic scales to produce the graph of the Biggest Fragment Size *vs* Second Moment which develop a boomerang profile where we have plotted the relative variance to identify regions with large density fluctuations due to critical behavior. This way critical behavior due to impact parameter increase or due to increase of the projectile energy can be easily seen by means of these plots.

Intermittency in fluctuations and correlations of a distribution has been employed to study turbulent flow, astrophysical phenomena and magnetohidrodynamics [23, 24]. This intermittency is shown in the self-similarity of large fluctuations that are not statistical on a large range of scales. To detect this behaviour, factorial moments are used that measure the properties of dynamical fluctuations without the bias of statistical fluctuations [25]. When this happens, factorial moments show a power law pattern with respect to the length of the subinterval in which the range of the studied variable is divided. This can be seen in terms of a linear relation between the logarithms of these quantities. Hence, Scaled Factorial Moments (SFM) can be used to detect a fluctuations intermittent pattern signed by a linear relation of ln(SFM) *versus* ln(δ). In this case, high density fluctuations will be self-similar in all the scales considered. SFM are given by:

$$F_i(\delta_s) = \left\{ \sum_{k=1}^{Z_{tot}/\delta_s} < n_k(n_k-1)\cdots(n_k-i+1) > \right\} /$$

$$\left\{ \sum_{k=1k}^{Z_{tot}/\delta_s} < n_k^i > \right\}, \quad i = 1,...,5. \tag{23}$$

A liquid-gas phase transition due to a spinodal decomposition in central heavy ion collisions can be shown by computing higher order charge correlations [13], given by:

$$\left. \frac{Y(\Delta Z, <Z>)}{Y'(\Delta Z, <Z>)} \right|_M, \tag{24}$$

where $Y(\Delta Z, <Z>)$ is equal to the number of fragments produced for given values of ΔZ and $<Z>$.

Spinodal decomposition is related to small density fluctuations spread out according to the following equation:

$$\frac{\partial n}{\partial t} = \nabla \cdot (M \nabla \mu), \tag{25}$$

where M is the moblity of the medium. The force that originates diffusion comes from the differences in the chemical potential for the perturbation and the chemical potential of the medium. Writing μ in terms of the free energy, diffusion equation can be generalized (once it is linearized with respect to n) as:

$$\frac{\partial n}{\partial t} = M \frac{\partial^2 f}{\partial n^2} \nabla^2 n - MB \nabla^4 n \, . \tag{26}$$

Describing an arbitrary fluctuation in terms of its Fourier components, the general solution of the last equation is an oscillatory function given by $\delta n = A(\vec{q}, t) \cos(\vec{q} \cdot \vec{r})$ whose width is given by:

$$A(\vec{q}, t) = A(\vec{q}, 0) \exp\left(-Mq^2 \left[\frac{\partial^2 f}{\partial n^2} + Bq^2 \right] t \right) . \tag{27}$$

Two possibilities arise, whether $\left(\dfrac{\partial^2 f}{\partial n^2} + Bq^2 \right) > 0$, for damped fluctuations, or $\left(\dfrac{\partial^2 f}{\partial n^2} + Bq^2 \right) < 0$, in which case the inhomogeneities will be exponentially amplified with time and a spinodal decomposition takes place.

Raduta et. al. have applied a microcanonical analysis and found that in the plot temperature .vs. excitation, when a spinodal instability happens the heat capacity is negative and there is a temperature plateau of 6.5 MeV[19].

Also, a plateau in the caloric curve has been associated with the liquid-gas phase transition, and the limit temperature in this plateau has been considered as inversely related with the residual size of the compound formed by the projectile and the target. These caloric curves are built computing the participant temperature obtained applying the kinetic gas temperature to the nucleons in the participant region:

$$E = \frac{m_f V_f^2}{2} = \frac{3}{2} n_f kT \, . \tag{28}$$

Several studies of the caloric curve in heavy ion collisions have shown that there is a size effect for the limit temperatures of these caloric curves [14]. Also, when isotopic temperatures are used to estimate the caloric curves, several kinds of shapes have been obtained [15]. These shapes can be growth-plateau-growth[16], growth-plateau [17], or even a growth-growth shape that lacks the plateau expected in the first order phase transition [18].

Excitation is computed as the temperature attained by the system at the the maximum compression of the compound formed by the projectile and the target.

An inverse relation between excitation and residual size is expected and in this article we confirm this expectation.

Once the collision dynamic simulation is performed, prompt fragments are detected, times when microscopic composition remains frozen are identified and excitation energy as well as temperature are computed, a caloric curve can be obtained. Fig. 15 shows the caloric curves computed for a wide energy range of excited collision systems. As can be seen, caloric curves are similar to those obtained from uniformly excited systems [20]. Once again, the relevant characteristic is the almost constant temperature behavior in fragmentation region. In other words, collision data provide a "rise-plateau" caloric curve. Besides, these caloric curves portray a limit temperature that diminishes as the residual size increases.

3. RESULTS

Clear criticality signals were obtained when the impact parameter is increased, for central Ni+Ni heavy ions collision. When the projectile energy is equal to 1 300 MeV, high values of the relative variance were obtained for large impact parameters with a relative variance peak attained when the impact parameter changes from 4 to 6fm (Fig. 7).
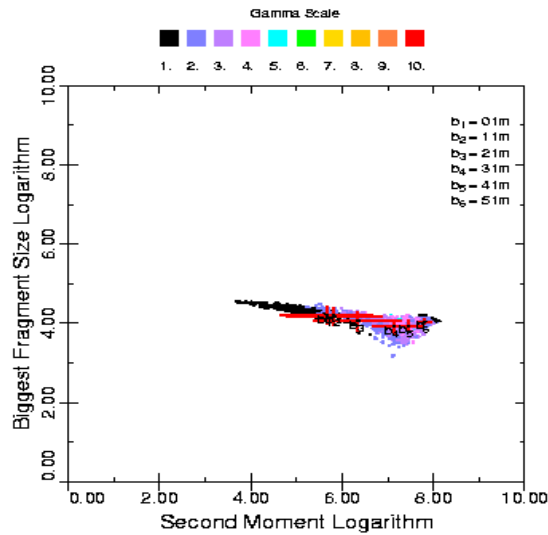

Fig. 7 – Campi Plot for Ni+Ni heavy ion collision with Eproy = 1 300 MeV simulated with LATINO Model.

Therefore, these signals indicate a phase transition induced by the increase of the impact parameter. This is confirmed in the Campi Plot with an impact

parameter equal to 4 fm and projectile energy varies from 900 to 2 000 MeV (Fig. 8). As portrayed in Fig. 8 large values of the relative variance are attained in the boomerang region of this graph.

A relative variance peak develops between 1 300 and 1 500 MeV. Critical region area is decreased when the impact parameter grows up to 5 fm as shown in Fig. 9, where scattered plot comes out to be a small area with high values of the relative variance. Relative variance attains a peak in the small boomerang vertex for several projectile energies in the range of 900 to 2 000 MeV. When impact parameter is increased, a three sources pattern is shown, namely a projectile, a target and an intermediate velocity source (Fig. 10). As shown in Fig. 10, this three sources pattern can be observed when a Ni+Ni collision with a projectile.
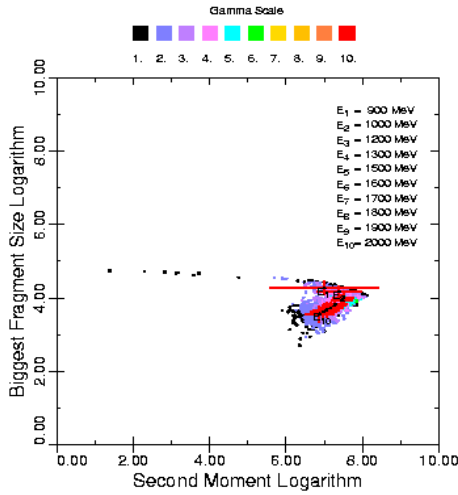
Fig. 8 – Campi plot for central Ni+Ni heavy ion collision with an impact parameter equal to 4 fm, simulated with LATINO Model.
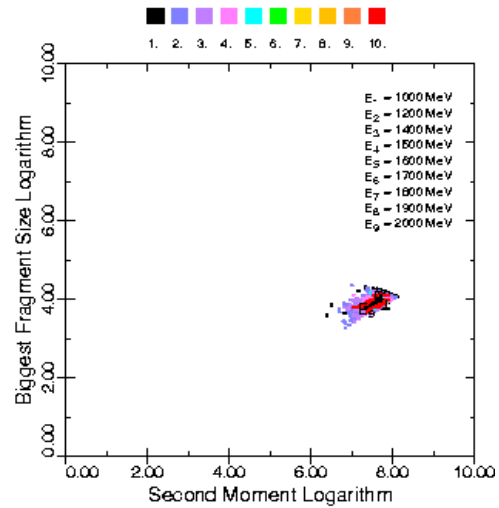
Fig. 9 – Campi Plot for central Ni+Ni heavy ion collision with an impact parameter equal to 5 fm, simulated with LATINO Model.

Projectile energy equal to 900 MeV and an impact parameter equal to 6 fm, is simulated with LATINO Model.

This suggests that a liquid-gas phase transition can be interpreted as the decomposition of the liquid phase made by the compound initially formed by the projectile and the target which decomposes into a phase formed by light particles that build the gas phase plus two remnants of the initial compound which are in the liquid phase.
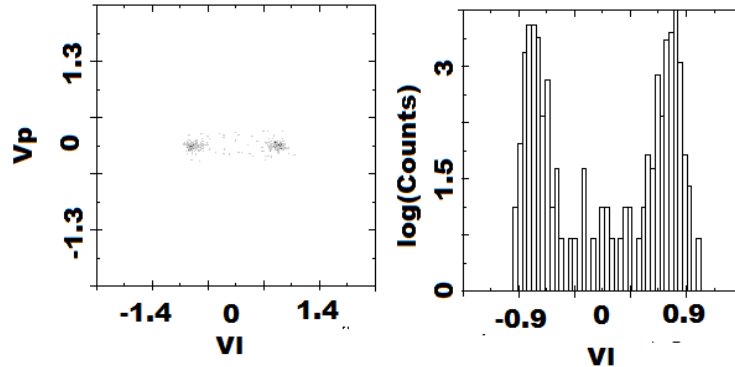
Fig. 10 – When impact parameter is high, a three sources is shown, namely a projectile,
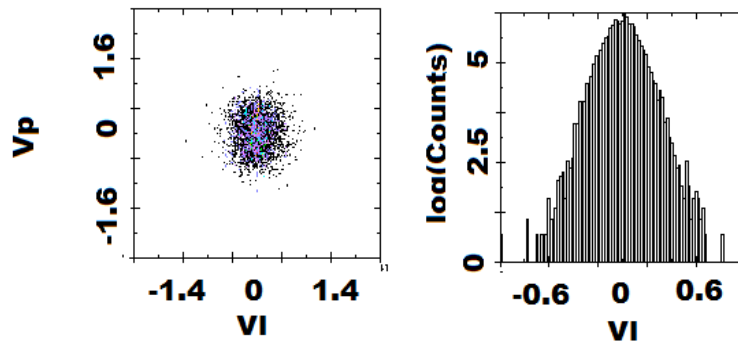a target and an intermediate velocity source.

Fig. 11 – When impact parameter is equal to zero, a one source pattern develops with fragments
emitted at intermediate velocities with a flow angle is in the range of 90 degrees. Ni+Ni collision
with a projectile energy equal to 900 MeV and an impact parameter equal to 0 fm, simulated
with LATINO Model.

This is in contrast to the pattern obtained when the collision is central
(Fig. 11), where a one source shape is shown and fragments are emitted at
intermediate velocities and with a flow angle equal to 90 degrees. For a large
impact parameter, light fragments are isotropically emitted from a source moving
at intermediate velocity, with a flow angle in the range of 18 degrees (Fig. 12),
which can be interpreted as a gas phase.

Scaled Factorial Moments Analysis was carried out for central Ni+Ni heavy
ion collisions when Eproy =1 300 MeV simulated with LATINO Model. showing
linear graphs that indicate self-similarity due to scaling (Fig. 13). This critical
behaviour happens in the same region of criticality shown by the Campi Plots,
confirming that in the critical region there are large density fluctuations as well as
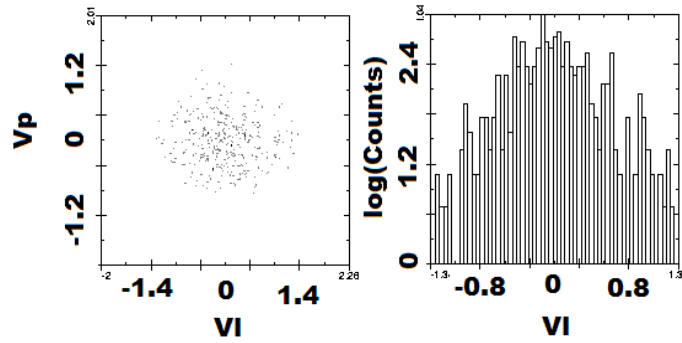self-similarity due to scaling.

Fig. 12 – When the impact parameter is high, fragments are emitted isotropically from a source moving at intermediate velocity and with flow angles in the range of 18 degrees. Ni+Ni collision at 1 000 MeV and 4fm, simulated with LATINO Model.
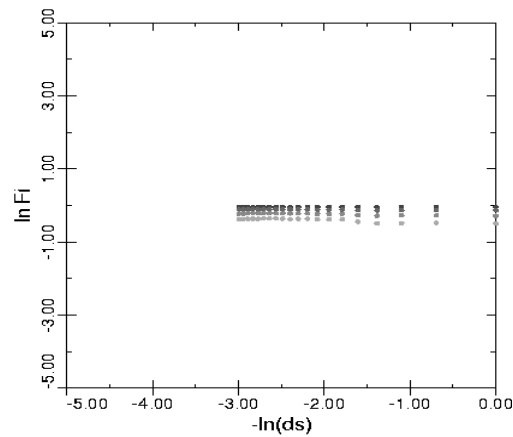

Fig. 13 – Scaled Factorial Moments Analysis for central Ni+Ni heavy ion collisions when Eproy = 1 300 MeV simulated with LATINO Model. Linear graphs indicate self-similarity due to scaling.

Higher order correlations show a peak for a fragment size equal to 6, with four equal sized fragments produced with this privileged size and an excitation equal to 4.75 MeV (Fig. 14). This peak can be considered a fossil spinodal decomposition signature given by an early breakup of equal sized fragments of a privileged size.

An inverse relation between excitation and residual size was obtained hereby as shown in Fig. 15 for Ag+Ag heavy ion collision. This suggests that when the residual is large we expect low temperatures since projectile energy and excitation are low. Also, when the projectile energies are large, larger temperatures will be experienced by the compound which should lead to larger excitations and since the

residual disassembles from the bulk, smaller residuals will be expected. Therefore we expect that excitation will decrease with residual size.
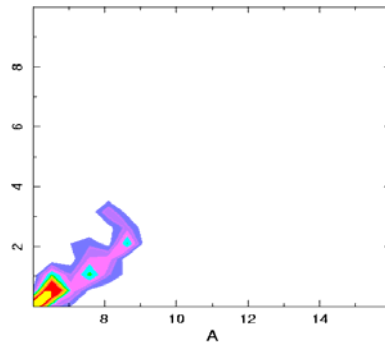

Fig. 14 – Higher order correlations show a peak for a fragment size equal to 6, with four equal sized fragments produced with this privileged size and an excitation equal to 4.75 MeV. Ni+Ni heavy ion central collision simulated with LATINO Model.

Also caloric curves were computed for central Ag+Ag heavy ion collisions using LATINO Model. Fig. 16 shows that limit temperatures decrease when the residual is increased.
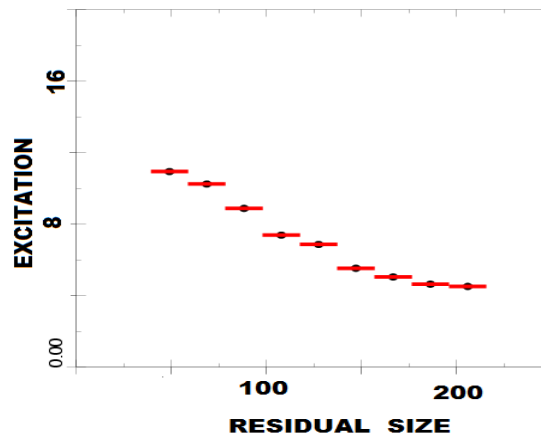

Fig. 15 – Excitation inversely correlated to the residual size. Ag+Ag central collisions simulated with LATINO Model.

4. CONCLUSION

Scaled Factorial Moments Analysis confirm the self-similarity expected in critical states such as a phase transition induced by an increase of impact parameter. This is signed by straight lines in the graph ln(dF) versus ln(ds).

Critical behavior of Scaled Factorial Moments Plots, indicate system entrance into a gaseous phase. In this case, a largest density fluctuation is in agreement with experimentally observed phase transitions.
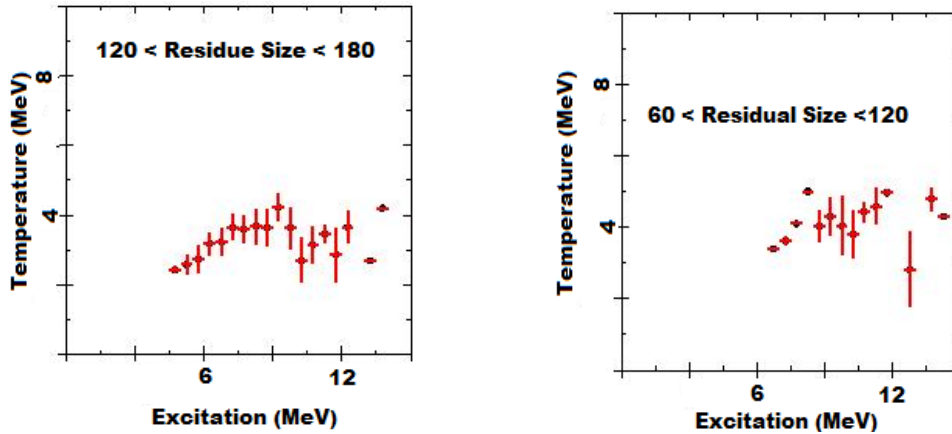

Fig. 16 – Caloric curves computed for central Ag+Ag heavy ion collisions using LATINO Model. Limit temperatures decrease when the residual is increased.

Signals suggest a phase transition induced by the increase of impact parameter. This is confirmed when Campi plots are examined and a relative variance peak appears when impact parameter is increased. Critical region is reduced when impact parameter is increased, with high relative variance values. Relative variance maximums are related with high density fluctuations. These instability signatures are associated with a phase transition, and confirmed by the self-similarity signature of a linear relation in the Scaled Factorial Moments plots. Caloric temperatures and excitation curves decrease with residual size in agreement with experimental results.

REFERENCES

1. J. D. Frankland *et al.*, *Multifragmentation of a very heavy nuclear system. 2. Bulk properties and spinodal decomposition*, Nucl. Phys. A, **689**, pp. 940-964, 2001.
2. L.G. Moretto and G.J. Wozniak, *Multifragmentation in Heavy-Ion Processes*, Ann. Rev. of Nuclear and Particle Science, **43**, pp. 379-455, 1993.

3. A. Guarnera *et al*., *3D stochastic mean-field simulations of the spinodal fragmentation of dilute nuclei*, Phys. Lett. B, **373**, pp. 267-274, 1996.

4. B. Borderie, G. Tabacaru, P.H. Chomaz, M. Colonna, A. Guarnera, M. Parlog, M. F. Rivet, The INDRA Collaboration, *Evidence for spinodal decomposition in nuclear multifragmentation,* Physical Review Letters, *15*, **86**, pp. 3252-3255, 2001.

5. A. Barrañón, J. Escamilla-Roa and J. A. López, *Entropy in the Nuclear caloric curve*, Physical Review C, *1*, **69**, pp. 1-6, 2004.

6. M. D'Agostino *et al*., *On the reliability of negative heat capacity measurements*, Nucl.Phys. A, **699**, pp. 795-818, 2002.

7. J.B. Elliott *et al*., *The liquid to vapor phase transition in excited nuclei*, Phys.Rev.Lett. **88**, 2002, 042701.

8. M. D'Agostino *et al*., *Thermodynamical features of multifragmentation in peripheral Au + Au Collisions at 35 A. MeV*, Nucl.Phys. A, **650**, pp. 329-357, 1999.

9. A. Barrañón, J. Escamilla-Roa and J. A. López, *The Transition Temperature of the Nuclear Caloric Curve*, Brazilian Journal of Physics, **34**, pp. 904-906, 2004.

10. A. Barrañón, A. Chernomoretz, C.O. Dorso, J. Lopez, and J. Morales, *Latino: A Semiclassical Model to Study Nuclear Fragmentation*, Rev. mex. de fisica, **45**, *2*, Oct. 1999.

11. R.J. Lenk, T.J. Schlagel and V.R. Pandharipande, *Accuracy of the Vlasov/Nordheim approximation in the classical limit*, Phys. Rev. C, **42**, pp. 372-385, 1990.

12. L. Verlet, *Computer Experiments on Classical Fluids. I. Thermodynamical Properties of Lennard-Jones Molecules,* Phys Rev., **165**, 201, 1967.

13. L. G. Moretto et. al., *Charge Correlations and Dynamical Instabilities in the Multifragment Emission Process*, Phys. Rev. Lett., **77**, pp. 2634–2637, 1996.

14. J. B. Natowitz, *et al*., *Caloric Curves and Critical Behavior in Nuclei*, Physical Review C, **65**, *3*, 034618, 2002.

15. V. Viola *et al*., *Double isotope-ratio thermometers: The influence of emission time scales*, Physical Review C, **59**, *5*, pp. 2660–2669, 1999.

16. J. Pochodzalla *et al*., *Probing the Nuclear Liquid-Gas Phase Transition*, PHYS. Rev. Lett., *6*, **75**, pp. 1040–1043, 1995.

17. V. Serfling *et al*., *Temperatures of Exploding Nuclei*, Phys. Rev. Lett., *18*, **80**, pp. 3928–3931, 1998.

18. J.A. Hauger *et al*., *Dynamics of the Multifragmentation of 1A GeV Gold on Carbon*, Phys. Rev. Lett., **77**, *2*, pp. 235–238, 1996.

19. l.H. Raduta, and R. Raduta, *Echos of the liquid-gas phase transition in multifragmentation*, Nucl. Phys. A, **703**, *3-4*, 876-888, 2002.

20. A. Strachan and C.O. Dorso, *Caloric curve in fragmentation*, Physical Review C, *2*, **58**, R632–R636, 1998.

21. D. Stauffer, *Scaling theory of percolation clusters*, Physics Reports, **54**, *1*, pp. 1-74, 1979.

22. X. Campi, *Signals of a phase transition in nuclear multifragmentation*, Phys. Lett. B, **208**, *3-4*, pp. 351-354, 1988.

23. B. Mandelbrot, *Intermittent turbulence in self-similar cascades: divergence of high moments and dimension of the carrier*, J. Fluid. Mech., **62**, pp. 331-358, 1974.

24. L.P. Kadanoff, *Scaling and universality in statistical physics*, Physica A, **163**, pp. 1-14, 1990.

25. A. Bialas and R. Peschanski, *Intermittency in multiparticle production at high energy*, Nuc. Phys. B, **308**, *4*, pp. 857-867, 1988.

26. Bao-An Li and S. Yenello, *Isospin nonequilibrium in heavy-ion collisions at intermediate energies*, Phys. Rev. C, **52**, *4*, R1746–R1749, 1995.